Energy-dependent carrier relaxation in self-assembled InAs quantum dots

H. S. Ling, C. P. Lee, and M. C. Lo

Citation: Journal of Applied Physics **103**, 124311 (2008); doi: 10.1063/1.2947599
View online: http://dx.doi.org/10.1063/1.2947599
View Table of Contents: http://scitation.aip.org/content/aip/journal/jap/103/12?ver=pdfcov
Published by the AIP Publishing

Energy-dependent carrier relaxation in self-assembled InAs quantum dots

H. S. Ling,[a] C. P. Lee, and M. C. Lo
Department of Electronic Engineering, National Chiao Tung University, 1001 Ta Hsueh Road, Hsinchu 300, Taiwan

(Received 24 November 2007; accepted 18 April 2008; published online 26 June 2008)

Selective excitation photoluminescence spectroscopy was employed to study InAs/GaAs self-assembled quantum dots (QDs). Under different excitation energies, different groups of QDs are selected and then emit light. The excited carriers relax to the ground state through different mechanisms when excited at different energies. Three distinct regions with different mechanisms in carrier excitation and relaxation are identified in the emission spectra. These three regions can be categorized from high energy to low energy, as continuum absorption, electronic state excitation, and multiphonon resonance. The special joint density of state tail of the QD that extends from the wetting layer band edge facilitates carrier relaxation and is posited to explain these spectral results.
 [DOI: 10.1063/1.2947599]

I. INTRODUCTION

Self-assembled quantum dots (QDs) grown on lattice mismatched material systems using the Stranski–Krastanov growth mode have been applied to various optoelectronic devices, including quantum dot lasers[1] and quantum dot infrared photodetectors.[2] The relaxation mechanism of carriers in such systems with discrete energy levels must be understood. Numerous efforts have been made in this area using various spectroscopic approaches.[3–12]

The energy relaxation of carriers in QDs cannot be simply achieved by the interaction between carriers and acoustic phonons because of the large separation between quantized energy levels. Other channels such as Auger-type scattering[13] and/or multioptical phonon scattering[14] are required to enable the relaxation process.

Under weak coupling conditions, Fermi's golden rule applies. Accordingly, the carrier relaxation through multioptical phonon scattering can be studied using photoluminescence (PL). The discreteness of the phonon energy and the inhomogeneity in the quantized energy levels of the QDs support the application of the selective excitation PL (SEPL) or PL-excitation (PLE) techniques to probe the energy spectrum of selected QDs and examine the carrier relaxation process, even though these approaches are basically time independent.

Carrier relaxations both with and without multioptical phonon "filtering" have been observed.[3–12] These two behaviors can be distinguished in the spectra because of the difference between the characteristics of the relaxation mechanisms. Without multiphonon filtering, the SEPL or the PLE spectra should reveal information on the energy levels of the QDs selected by resonant excitation. In contrast, if the relaxation undergoes multiphonon filtering, such that only the QDs with relaxation energies equal to multiphonon energies can emit light, then the spectra instead reveal certain longitudinal optical (LO) phonon replicas. For those filtered out QDs, which do not satisfy multiphonon energy conservation, the excited carriers cannot relax to the ground state but are depleted either through nonradiative recombination[12] or through excited-state emission. The two aforementioned phenomena have been observed from different samples by different research groups.[3–12] However, the inter-relationship between these two phenomena and the detailed mechanism of the efficient carrier relaxation between QDs' discrete states that bypasses LO phonon filtering are still unclear.

In this study, carrier relaxation with and without LO phonon filtering were both observed from a single sample with different excitation energies. For the first time, this energy-dependent relaxation mechanism is investigated and explained.

II. SAMPLES AND EXPERIMENTS

The QD samples used herein were grown using a Veeco GEN-II molecular beam epitaxy system with a valved cracker As cell on (001) semi-insulating GaAs substrates. A single InAs QD layer with 150 nm GaAs barrier layers and an additional surface QD layer for atomic force microscope (AFM) measurement were grown in each sample. Two samples with QDs of different sizes were prepared. In sample A, large QDs were purposefully grown. 2.6 ML of InAs with a 0.05 μm/h growth rate were deposited at 520 °C under As_2 flux. However, for sample B, ultrasmall QDs were prepared with 2.4 ML of InAs grown at a rate of 0.1 μm/h and a lower growth temperature of 480 °C. As_4 atmosphere (the cracking zone of the As cell was set to 500 °C) at a pressure of 1.5×10^{-5} Torr was used to minimize the probability of coalescence of the QDs. The layers except the regions near QDs were grown at around 600 °C to ensure the growth of high-quality epilayers. Figures 1(a) and 1(b) present AFM images of samples A and B, respectively. The AFM data reveal that the lens-shaped QDs in sample A had an average height of 9 nm and an average diameter of 47 nm. The density of the dots was about 2×10^{10} cm^{-2}. In sample B, the QDs were very small and dense [Fig. 1(b)]. The average dot height and the average base diameter were about 1.5 and 17 nm, respectively; the density reached 1.2×10^{11} cm^{-2}. The SEPL and the PLE

[a]Author to whom correspondence should be addressed. Electronic mail: karshe.ee92g@nctu.edu.tw. Tel.: +886-3-5712121-54248. FAX: +886-3-5733722.

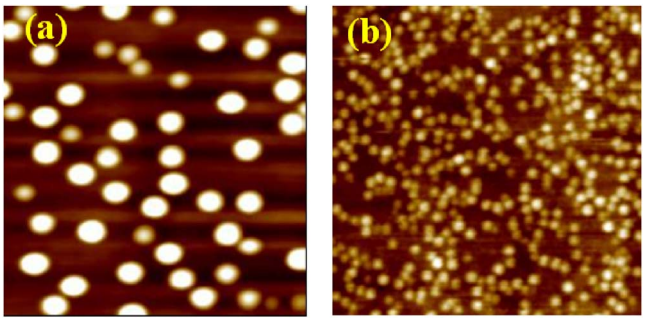

FIG. 1. (Color online) 500 nm squared AFM images of (a) sample A and (b) sample B.

spectra of the QDs were measured using a Ti:sapphire laser that was pumped with an argon ion laser, while the conventional PL (or nonresonant PL) spectrum was obtained directly using the argon ion laser. The sample was mounted in a close-cycled helium cryostat for low-temperature measurement. Since the QDs in the two samples are of different sizes, the samples exhibit different ground state transition energies. At 13 K, the emission peaks of samples A and B were at 1.168 and 1.269 eV, respectively.

III. DISCUSSIONS

The SEPL spectra of sample A, shown in Fig. 2, were obtained as the excitation energy was varied from 1.378 to 1.211 eV. (The spectra are arranged with decreasing energy from top to bottom.) The excitation energy for each spectrum is marked by a cross on the right-hand side. All excitation energies were below the wetting layer (WL) ground state energy (which was approximately 1.45 eV, as determined from the high-power PL spectrum shown in the inset) to ensure that only the QD layer could absorb the pumping photons. The excitation power was around 1 W/cm^2, which was purposely chosen to be low enough to avoid any emission from an excited state and to suppress Auger scattering. When the excitation energy (E_{ex}) exceeds 1.34 eV, the luminescence spectra show a broad peak, indicating that all QDs are excited. As the excitation energy decreases, fine structures with narrower peaks are observed because of the selective excitation of QDs with specific sizes that allow carrier relaxation through discrete energy levels.

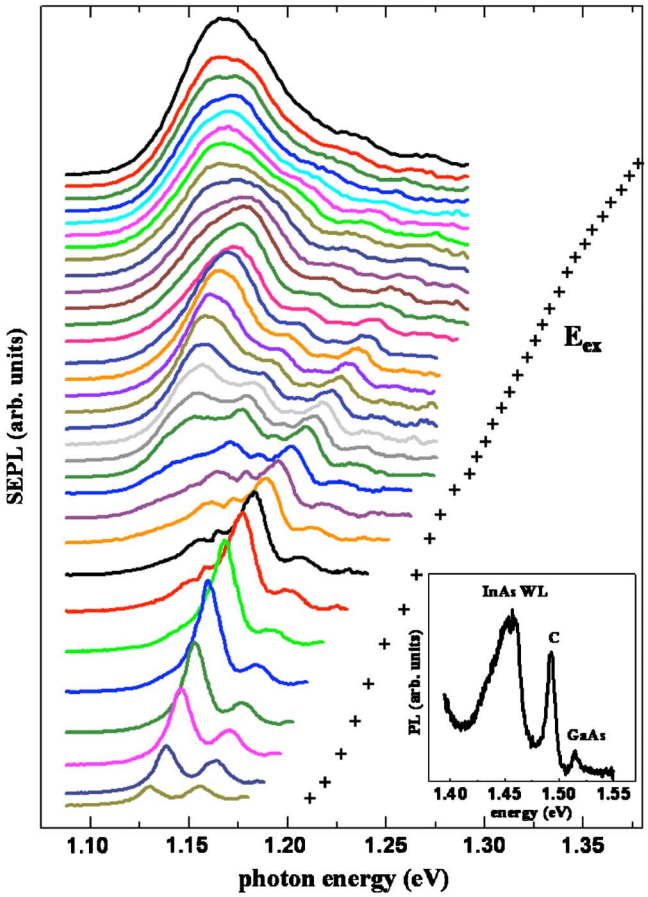

FIG. 2. (Color online) SEPL spectra of large QDs (sample A) obtained at 13 K. The cross on the right-hand side of each spectrum indicates the excitation energy. The inset shows the high-power PL spectrum.

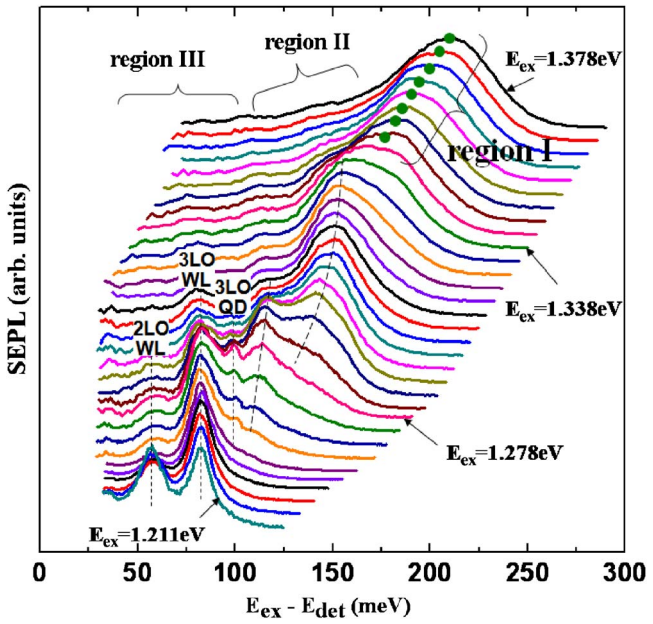

FIG. 3. (Color online) SEPL spectra of sample A with normalized intensity as a function of the relaxation energy ($E_{ex}-E_{det}$). The three regions I, II, and III correspond to different excitation and relaxation mechanisms.

The spectra obtained in Fig. 2 are better understood by plotting them as functions of relaxation energy, $E_{ex}-E_{det}$, which is the difference between the excitation energy and the emission energy of each QD. This plot in Fig. 3 reveals three distinct regions. At the low end of the excitation energy, the sharp peaks in the bottom few spectra lineup vertically in the same positions. The peak values of $E_{ex}-E_{det}$ correspond exactly to particular multi-LO phonon energies, suggesting that only the QDs with excited states at multiple phonon energies above their ground state are selectively excited. At the high end of the excitation energy, with energies of over about 1.338 eV, only one broad peak (indicated by the filled circle) is observed in each spectrum. These broad peaks have the same emission energy as in the conventional PL spectrum, suggesting that all the QDs are excited and participate in the light emission. When the excitation energy is in the middle range, a different excitation scheme is observed. Both the emission energy (Fig. 2) and $E_{ex}-E_{det}$ (Fig. 3) of the selective excited QDs vary continuously with the excitation energy. The sharp peaks associated with selective excitation via

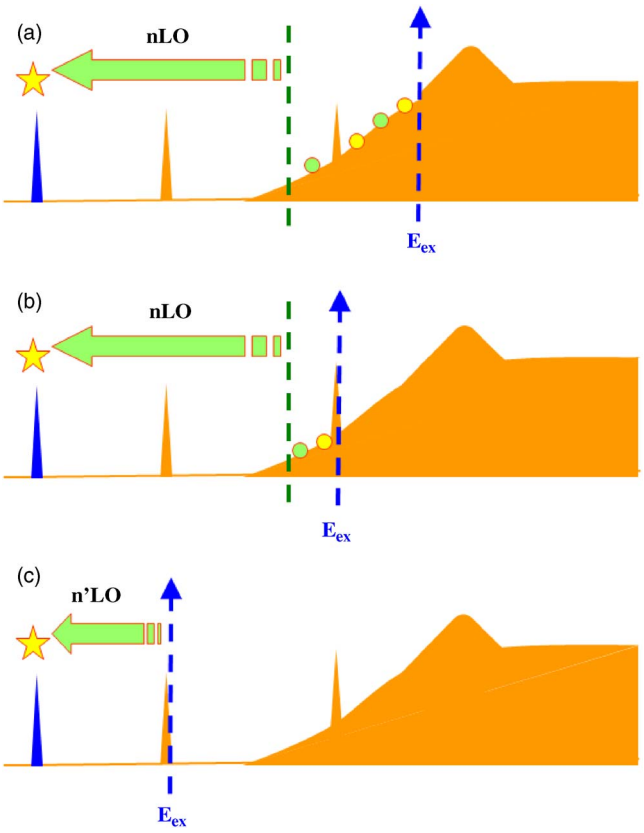

FIG. 4. (Color online) The schematic relaxation processes associated with (a) region I, (b) region II, and (c) region III in Fig. 3.

a multi-LO phonon process are no longer there, but the broad emission peak observed at high excitation energies is also absent. As will be discussed in the following, the quantized energy levels in the selected QDs are responsible for the emission spectra in this energy range.

The three distinct regions in the PL spectra under various excitation energies are designated as regions I, II, and III (from high to low energy). The origin of these three regions is explained by the different excitation and carrier relaxation mechanisms as follows. The pioneering work of Toda *et al.*[15] demonstrated the existence of a continuum of tail states below the WL band edge in the PLE spectrum of a single QD. Vasanelli *et al.*[16] explained that such a broad band is the result of the crossed transitions between the discrete states in the QD and the continuum states in the WL. The joint densities of states between the localized and the delocalized states give rise to the continuous background in the excitation spectrum of the QD.

In Fig. 4, we plot qualitatively the joint densities of states of a QD to understand the observed energy-dependent spectra. The diagrams present three discrete states, with the uppermost state lying within the continuum tail. The positions of the excitation energy and the emission energy (lowest discrete state) in the three different situations described above are also indicated. Figures 4(a)–4(c) explain the excitation and relaxation schemes for regions I, II, and III in Fig. 3.

When E_{ex} is lower than the WL peak but higher than the discrete states of the QD, as shown in Fig. 4(a), the excited carriers can relax to the ground state by rolling down the continuum tail (through acoustic phonon emission) and then cascading through multi-LO phonon emission. Because the excitation energy that lies within the continuum tail generates a localized electron/hole in the QD and a free carrier with an opposite charge in the WL, the free carrier can be readily captured by the QD due to a Coulomb attraction. Hence the relaxation of excited carriers is efficient in this regime. Moreover, through quasicontinuous absorption, all of the QDs are excited, although the E_{ex} is lower than the WL band edge. Therefore, under this excitation condition (region I or high-energy excitation), all of the QDs emit light and the emission spectra are basically the same as that from conventional PL measurement.

The density of states associated with the continuum tail declines gradually as the energy decreases. Once the excitation energy of the pumping photons is sufficiently low to reach the discrete states of the QD, the sharp levels enhance absorption by resonant excitation. At moderate excitation energies (region II in Fig. 3), the carriers are resonantly excited to the upper discrete states, which lie within the continuum tail of the joint densities of states. As shown in Fig. 4(b), in addition to the multi-LO phonon scattering, the relaxation of the excited carriers can still be achieved via the continuum states. The QDs whose upper states resonate with the excitation energy thus yield ground state emission. In this case, the energies of the discrete states of the QDs can be extracted from the spectra. Since the QDs are inhomogeneous not only in size but also in shape and alloy profile, the emission energy of the resonantly excited QDs may still have a distribution. Therefore, the observed emission peak is not as narrow as that from a single QD.

Notably, the continuum in the joint density of states arises from the continuous states above the WL band edge either of the conduction band or of the valence band. Once an electron-hole pair has been excited into a state within the continuum, the energy of this pair can be relaxed through the continuous states by either the electron or the hole. This is basically the energy relaxation mechanism associated with regions I and II in Fig. 3. The difference between the two, however, is in the selective excitation process in region II, which is governed by the sharp peaks associated with the discrete energy levels that overlap the continuum in the joint density of states. The enhanced absorption due to these peaks selectively excites the QDs whose peaks resonate with the excitation energy. These resonantly excited electron-hole pairs can undergo electron-hole scattering[17] and then release energy through continuous states in either the conduction band or the valence band. Since the quantized energy levels in QDs are functions of their size, information can be gained from the size-dependent energy levels of the QDs in the spectra in region II.

At very low excitation energies, as shown in Fig. 4(c), when the carriers are resonantly excited to states below the continuum tail, they can relax to the ground state only via a multiphonon process. The sharp peaks in the bottom few emission spectra in Fig. 3 (region III) are therefore signatures of the multi-LO phonon filtered relaxation. These phonon resonant peaks have been confirmed to arise from an excited-state absorption followed by multiphonon relaxation but not

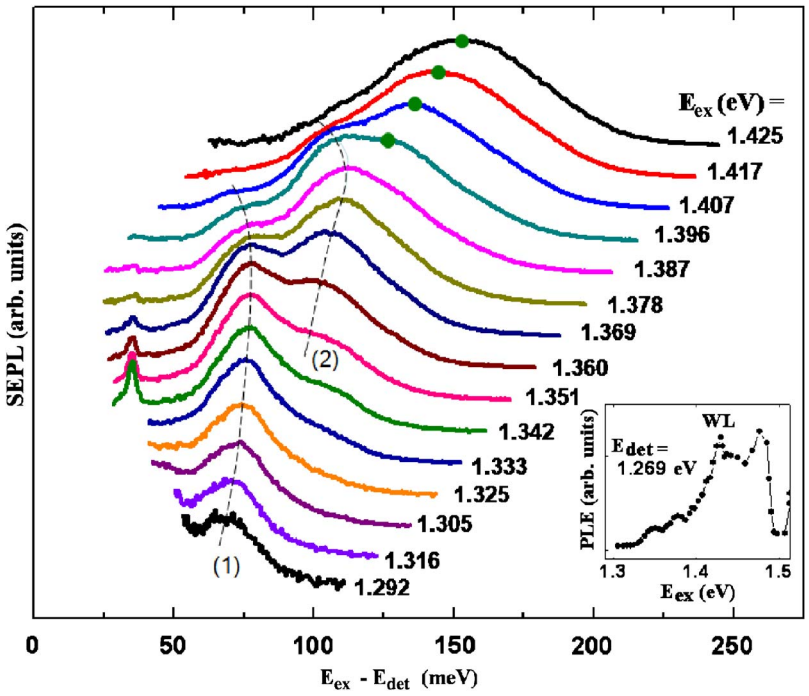

FIG. 5. (Color online) SEPL spectra of small QDs (sample B) at 13 K. The x-axis refers to $E_{ex}-E_{det}$ and the intensity of each spectrum is normalized for clarity. The inset displays the PLE spectrum with the detection energy fixed at 1.269 eV.

from a resonant Raman process.[11] The emission peaks in region III are even narrower than those in region II because the selected QDs need to be consistent with not only resonant absorption but also a multiphonon resonant relaxation. Three phonon lines, marked by vertical straight lines in Fig. 3, are ascribed, from left to right, to the 2LO WL phonon peak (56 meV), the 3LO WL phonon peak (83 meV), and the 3LO QD phonon peak (100 meV). These assignments yield the energy of the WL phonon as ~27.8 meV and that of the QD phonon as ~33.3 meV. These values are very close to those obtained by Steer *et al.*,[9] which were ~28.4 meV as the WL phonon energy and ~34 meV as the QD phonon energy. The value for the WL phonons is lower than the LO phonon energy of the bulk InAs, 29.9 meV, because of the strong phonon confinement in the thin WL; the higher phonon energy for the QDs follows from the strong strain effect associated with the QDs.[10]

The distribution of the joint density of states and the relative positions of the discrete states to the continuum are functions of the QD size. As the QDs become smaller, their discrete states move to the high-energy side faster than the continuum, so they may lie deeper in the continuum tail.[16] In this case, the energy relaxation of carriers via the continuum is more pronounced. The SEPL study of sample B, which has extremely small QDs, was also conducted. Figure 5 displays the spectra of sample B that are plotted versus $E_{ex}-E_{det}$. The peak intensity is also normalized for clarity. All excitation energies were below the WL band edge, which was 1.43 eV (as determined from the PLE spectrum in the inset). The shapes of the upper few spectra are similar to those of region I in Fig. 3. Hence, the carriers were excited to the continuum portion of the density of states. When the excitation energy is lower than 1.41 eV, two resonant peaks are observed [see guided lines (1) and (2)]. The fact that they do not line up at the same horizontal positions suggests that energy relaxation proceeds not only via the multi-LO phonon process, as in region III in Fig. 3. Rather, the process is of the type associated with region II in Fig. 3. This result confirms the continuum tail assisted relaxation under resonant excitation in such a sample with small QDs. Figure 5 also includes another very sharp peak at $E_{ex}-E_{det}=35$ meV. The particularly small peak width (~2 meV) suggests a resonant Raman process, in which the carriers are directly excited to the ground state of the QDs. The characteristic peak energy, 35 meV, suggests that this Raman process is associated with the interface phonons in the QD structure.[10,18]

Since the relaxation process in sample B need not meet the multi-LO phonon resonance condition, size-dependent excited-state separations can be obtained by plotting the relaxation energy ($E_{ex}-E_{gs}$) versus the ground state energy (E_{gs}) for the two resonant peaks in Fig. 5. Figure 6 is such a plot, and it demonstrates that $E_{ex}-E_{gs}$ initially increases with E_{gs} but then declines. For the QDs with an E_{gs} of lower than about 1.28 eV, the increased excited-state separations exhibit a typical quantum size effect. However, for the small dots whose ground state energies exceed 1.28 eV, the quantum shape effect masks the quantum size effect.[7] In other words, these small QDs have a much lower height-to-width aspect ratio. This finding is expected because in the early stage of Stranski–Krastanov island growth, the deposited atoms do not support three dimensional growth until the nucleation sites are completely formed. Figure 6 also plots the size distribution of QDs in sample B, which is represented by the PL spectrum (dash line). For the most populated QDs, in which the ground state energy is 1.269 eV; the first excited state is separated by an energy separation of 77 meV from it, and the second excited state is separated by another 32 meV. Given the relaxed transition selection rule in nonsymmetrical self-assembled QDs, we believe that the large energy separation of 77 meV is associated with that between the e_0 state and the e_1 state. The small energy separation of 32 meV, on the

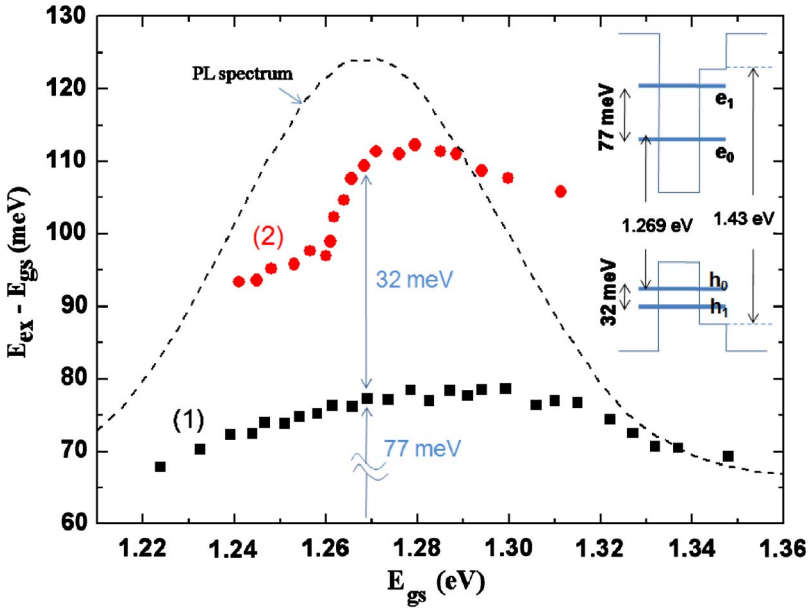

FIG. 6. (Color online) The relaxation energy as a function of the ground state energy for the two resonant peaks in Fig. 5. The dashed line is the PL spectrum of the sample showing the size distribution of the QDs. The band diagram in the inset is constructed for the most populated QDs.

other hand, follows from that between the h_0 state and the h_1 state. The possible band diagram for the most populated QDs is then constructed, as shown in the inset. Assuming that 70% band gap locates at the conduction band, this band diagram indicates that 48 meV is required to delocalize the bound holes in the h_0 state. Accordingly, when the h_0 hole and the e_1 electron are generated by the first excited-state excitation, the e_1 electron first releases energy to enter the e_0 state by transferring 77 meV to the h_0 hole and making the hole free. The free hole can then release energy easily through the continuous states in the valence band. Therefore, the relaxation of carriers from this resonant excitation is not restricted by particular LO phonon energies. Similarly, the relaxation of carriers from the second excited-state excitation proceeds even easier because the energy transfer from the e_1 electron is evidently sufficient to delocalize the h_1 hole. This band diagram thus verifies the possibility of continuum tail assisted relaxation described in Fig. 4(b).

IV. CONCLUSIONS

The energy spectra of InAs/GaAs self-assembled QDs were investigated using SEPL. The dependence of the emission spectra on the excitation energy provides important information about the carrier relaxation mechanism. Three distinct regions can be identified as associated with changes in the excitation energy. At high excitation energies, all QDs are excited and participate in the light emission with the help of the continuum states. At low excitation energies, the absence of the continuum states is such that the carrier relaxation is restricted to a multi-LO phonon process. Only the QDs with excited states at particular multi-LO phonon energies above the ground state can absorb and emit light. At medium energy, the QDs are resonantly excited through discrete electronic states, but the relaxation of the carriers does not need to meet the multiphonon resonance condition with the help of a continuum tail. For these resonantly excited electron-hole pairs, intradot electron-hole scattering provides an efficient channel for the release of energy via the continuous states of either electrons or holes.

ACKNOWLEDGMENTS

This work was financially supported by the National Science Council under Contract No. NSC 94-2215-E-009–010 and the ATU program of the Ministry of Education under Contract No. 95W803.

[1]M. Grundmann, Physica E (Amsterdam) **5**, 167 (2000).
[2]S. Chakrabarti, A. D. Stiff-Roberts, P. Bhattacharya, S. Gunapala, S. Bandara, S. B. Rafol, and S. W. Kennerly, IEEE Photonics Technol. Lett. **16**, 1361 (2004).
[3]S. Fafard, D. Leonard, J. L. Merz, and P. M. Petroff, Appl. Phys. Lett. **65**, 1388 (1994).
[4]Q. Xie, P. Chen, A. Kalburge, T. R. Ramachandran, A. Nayfonov, A. Konkar, and A. Madhukar, J. Cryst. Growth **150**, 357 (1995).
[5]K. H. Schmidt, G. Medeiros-Ribeiro, M. Oestreich, P. M. Petroff, and G. H. Dohler, Phys. Rev. B **54**, 11346 (1996).
[6]R. Heitz, O. Stier, I. Mukhametzhanov, A. Madhukar, and D. Bimberg, Phys. Rev. B **62**, 11017 (2000).
[7]M. Bissiri, G. Baldassarri Höger von Högersthal, M. Capizzi, P. Frigeri, and S. Franchi, Phys. Rev. B **64**, 245337 (2001).
[8]S. Farfad, R. Leon, D. Leonard, J. L. Merz, and P. M. Petroff, Phys. Rev. B **52**, 5752 (1995).
[9]M. J. Steer, D. J. Mowbray, W. R. Tribe, M. S. Skolnick, M. D. Sturge, M. Hopkinson, A. G. Cullis, C. R. Whitehouse, and R. Murry, Phys. Rev. B **54**, 17738 (1996).
[10]R. Heitz, M. Grundmann, N. N. Ledentsov, L. Eckey, M. Veit, D. Bimberg, V. M. Ustinov, A. Yu. Egorov, A. E. Zhukov, P. S. Kopev, and Zh. I. Alferov, Appl. Phys. Lett. **68**, 361 (1996).
[11]R. Heitz, M. Veit, N. N. Ledentsov, A. Hoffmann, D. Bimberg, V. M. Ustinov, P. S. Kopev, and Zh. I. Alferov, Phys. Rev. B **56**, 10435 (1997).
[12]R. Heitz, M. Veit, A. Kalburge, Q. Xie, M. Grundmann, P. Chen, N. N. Ledentsov, A. Hoffmann, A. Madhukar, D. Bimberg, V. M. Ustinov, P. S. Kopev, and Zh. I. Alferov, Physica E (Amsterdam) **2**, 578 (1998).
[13]U. Bockelmann and T. Egeler, Phys. Rev. B **46**, 15574 (1992).
[14]T. Inoshita and H. Sakaki, Phys. Rev. B **46**, 7260 (1992).
[15]Y. Toda, O. Moriwaki, M. Nishioka, and Y. Arakawa, Phys. Rev. Lett. **82**, 4114 (1999).
[16]A. Vasanelli, R. Ferreira, and G. Bastard, Phys. Rev. Lett. **89**, 216804 (2002).
[17]Al. L. Efros, V. A. Kharchenko, and M. Rosen, Solid State Commun. **93**, 281 (1995).
[18]Yu. A. Pusep, G. Zanelatto, S. W. da Silva, J. C. Galzerani, P. P. Gonzalez-Borrero, A. I. Toropov, and P. Basmaji, Phys. Rev. B **58**, R1770 (1998).